International Journal of Engineering Research
Volume No.3, Issue No.3, pp : 172-176
ISSN:2319-6890)(online),2347-5013(print)
01 March 2014

Optimizing InAs/InP (113) B quantum dot lasers with considering mutual effects of coverage factor and cavity length on two-state lasing

Saeed yazdani, Esfandiar Rajaei, Azam Shafieenezhad

Department of Physics,University of Guilan, Rasht, Iran

yazdani.saeed1988@gmail.com

Abstract—The optical gain and output power of quantum dot (QD) lasers with different coverage factors and cavity lengths have been investigated as a function of injection current that show differences lasing from the ground state (GS) and exited state (ES) and in order to compare numerical results for turn on delay we have calculated photon density for ground state.

Keywords— **Cavity length, Coverage factor, Output Power, Quantum dot lasers, Rate equations**

I. Introduction

While the first quantum-dot (QD) laser was developed about 20 years ago, the performance of QD lasers have improved significantly. Currently, compared to the conventional quantum-well (QW) lasers, QD lasers have shown extremely low threshold current, high internal efficiency, and superior characteristic temperature [i]–[vi]. However, the high-speed modulation performance of QD lasers is generally poorer compared to that of QW lasers due to several factors, such as the low carrier capture/relaxation rate and the closely spaced hole energy states in the QDs.

Semiconductor lasers with QD based active regions have generated a huge amount of interest for applications including communications networks due to their anticipated superior physical properties due to three dimensional carrier confinement. For example, the threshold current of ideal quantum dots is predicted to be temperature insensitive [vii]. Intensive attention should be paid to investigate the carrier dynamics in QD laser active regions. The carriers injected into the wetting layer (WL) are captured by QD ES with a relatively fast capture time of about several picoseconds. Then carriers relax into QD GS through some complicated dynamical processes. Especially, how the inter-level relaxation affects QD laser performance is very important for device design. Due to the photon bottleneck effect [viii], [ix], which is much slower than 0.1–1 ps in QWs [x]. This effect will have significant impact on the stimulated emission in QD lasers [xi]. Most investigations reported in the literature deal with In(Ga)As QDs grown on GaAs substrates [xii],[xiii]. In order to reach the standards of long-haul transmissions, 1.55 µm InAs QD lasers on InP substrate have been developed. Recent experimental studies conducted on these devices have shown that a second laser peak appears in the laser spectrum as the injection power increased. The double laser emission is a common property found independently by different research groups for In(Ga)As/GaAs as well as for InAs/InP (113)B systems [xiv]–[xv]. Many studies have been done on the simulation of spectral behavior and dynamic characteristics of self-assembled QD lasers [xvii]–[xxi].

At first we discuss energy levels in laser cavity and transitions between states. Then we describe rate equations and relations. After that, there are numerical calculations with figures and their explanations. Finally we there is conclusion part with a summary how to combine coverage factor and cavity length to provide a high quality optimizing for InAs/InP (113) B QD lasers. All these recent results will be reviewed later in the Paper.

II. Material and Methodology

In this section, in the following, a numerical model is used to study carrier dynamics in the two lowest energy levels of an InAs/InP (113) B QD system. Its active region consists of a QD ensemble with different dots interconnected with the WL. For simplicity, the existence of higher ESs is neglected and a common carrier reservoir is associated to both the WL and the barrier. The QD are assumed to be always neutral and electrons and holes are treated as eh-pairs and thermal effects and carrier losses in the barrier region are not taken into account. Fig. 1 shows a schematic representation of the carrier dynamics in the active region. First, an external carrier injection fills directly QD ensemble with a capture time (τ_{ES}^{WL}). Once on the ES, carriers can relax on the GS (τ_{GS}^{ES}), be thermally reemitted in the WL reservoir (τ_{WL}^{ES}) or recombine spontaneously with a spontaneous emission time (τ_{ES}^{spon}) or by stimulated emission of photons with ES resonance energy. The same dynamic behavior is followed for the carrier population on the GS level with regard to the ES.

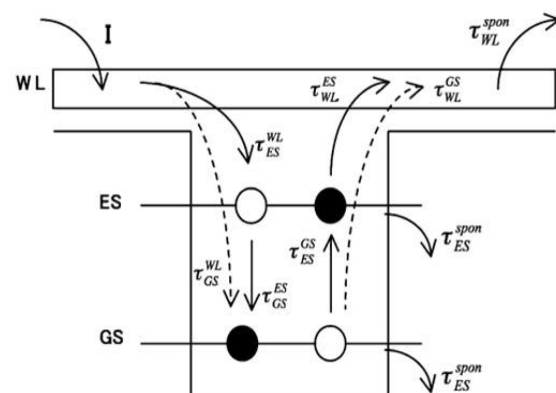

Fig.1: Schematic representation of the carrier dynamics model with direct relaxation channel (dashed line).

This approach has been previously developed for the InAs–GaAs system but in the case of InAs/InP (113) B system it is assumed that at low injection rates, the relaxation processes are phonon-

assisted while the Auger effect dominates when the injection gets larger. In order to include this effect, a modified model has been considered introducing a direct relaxation channel (τ_{GS}^{WL}) to the standard cascade relaxation model, as shown in Fig. 1 (dashed line). It is attributed to a single Auger process involving a WL electron captured directly into the GS by transferring its energy to a second WL electron. Carriers are either captured from the WL reservoir into the ES or directly into the GS within the same time $\tau_{GS}^{WL} = \tau_{ES}^{WL}$.

This assumption has been made after analysis of the kinetic curves in where the ES and GS population gave raise simultaneously curves in where the ES and GS population gave raise simultaneously 10 ps after excitation. On the other hand, carriers can also relax from the ES to the GS. The other transition mechanisms remain the same as in the cascade model. The capture and the relaxation times are then calculated through a phenomenological relation depending on the carrier density in the WL reservoir, the ES and GS occupation probabilities, and the existence probability of the ES and GS transitions.

$$\tau_{ES}^{WL} = \frac{1}{A_w + C_w N_w} \quad (1)$$

$$\tau_{GS}^{ES} = \frac{1}{A_E + C_E N_w} \quad (2)$$

Where N_w is the carrier number in the WL reservoir and A_w, A_E , C_w and C_E are the coefficients for phonon and Auger-assisted relaxation, respectively, related to the WL and the ES.

The eh-pairs escape times have been derived considering a Fermi distribution for the ES and GS carriers for the system in quasi-thermal equilibrium without external excitation. To ensure this, the carrier escape time is related to the carrier capture time as follows:

$$\tau_{GS}^{ES} = \tau_{ES}^{GS} \left(\frac{D_{GS}}{D_{ES}}\right) exp^{\frac{(E_{ES}-E_{GS})}{K_B T}}$$

(3)

$$\tau_{WL}^{ES} = \tau_{ES}^{WL} \left(\frac{D_{ES}}{\rho_{WL}}\right) exp^{\frac{(E_{WL}-E_{ES})}{K_B T}}$$

(4)

$$\tau_{WL}^{GS} = \tau_{GS}^{WL} \left(\frac{D_{GS}}{\rho_{WL}}\right) exp^{\frac{(E_{WL}-E_{GS})}{K_B T}}$$

(5)

Where ρ_{WL} is the effective density of states in the WL and E_{WL} is its emission energy and D_{ES} and D_{GS} are the degeneracy of the considered confined states.

The numerical model is based on the rate equations analysis is already reported for multimode state. According to all those assumptions, for one-mode state, describing the change in carrier number of the three electronic energy levels, can be written as [xxi]:

$$\frac{dN_{wL}}{dt} = \frac{I}{e} + \frac{N_{ES}}{\tau_{WL}^{ES}} - \frac{N_{WL}}{\tau_{ES}^{WL}}(1-P_{ES})$$

$$-\frac{N_{WL}}{\tau_{WL}^{spon}} - \frac{N_{WL}}{\tau_{gs}^{WL}}(1-P_{GS}) + \frac{N_{ES}}{\tau_{WL}^{GS}} \quad (6)$$

$$\frac{dN_{ES}}{dt} = \frac{N_{WL}}{\tau_{ES}^{WL}}(1-P_{ES}) + \frac{N_{GS}}{\tau_{ES}^{GS}}(1-P_{ES})$$

$$-\frac{N_{ES}}{\tau_{WL}^{ES}} - \frac{N_{ES}}{\tau_{GS}^{ES}}(1-P_{GS}) - \frac{N_{ES}}{\tau_{ES}^{SPON}}$$

$$-(\Gamma Vgk_{ES})(2P_{ES}-1)\left(\frac{s_{ES}}{1+\varepsilon_{ES}s_{ES}}\right) \quad (7)$$

$$\frac{dN_{GS}}{dt} = \frac{N_{ES}}{\tau_{GS}^{ES}}(1-P_{GS}) - \frac{N_{GS}}{\tau_{ES}^{GS}}(1-P_{ES})$$

$$-\frac{N_{QS}}{\tau_{GS}^{spon}} - (\Gamma V_g k_{GS})(2P_{GS}-1)\frac{S_{GS}}{1+\varepsilon_{GS}S_{GS}}$$

$$+\frac{N_{WL}}{\tau_{GS}^{WL}}(1-P_{GS}) - \frac{N_{GS}}{\tau_{WL}^{GS}} \quad (8)$$

With being the carrier number in the WL and the optical confinement factor. P_{GS} and P_{ES} are the filling probabilities of the ES and GS

$$P_{GS,ES} = N_{GS,ES} / D_{GS,ES}\, N_D \quad (9)$$

With $N_{GS,\,ES}$ being the GS and ES carrier numbers and N_D is surface density of QDs, D_{GS} is twofold degenerate (D_{GS}=2) and D_{ES} is fourfold degenerate (D_{ES}=4). In order to calculate the entire emission spectrum, the model has been extended considering also the presence of many cavity longitudinal modes, hence the photon number with resonant energy of the mode is depicted by

$$\frac{dS_{ES}}{dt} = (\Gamma V_g k_{ES})(2P_{ES}-1)\left(\frac{s_{ES}}{1+\varepsilon_{ES}s_{ES}}\right) - \frac{S_{ES}}{\tau_p} + \beta_{sp}\frac{N_{ES}}{\tau_{ES}}$$

(10)

$$\frac{dS_{GS}}{dt} = (\Gamma V_g k_{GS})(2P_{GS}-1)\left(\frac{s_{GS}}{1+\varepsilon_{GS}s_{GS}}\right) - \frac{S_{GS}}{\tau_p} + \beta_{sp}\frac{N_{GS}}{\tau_{GS}}$$

(11)

The material gain is described by the set of equations:

$$g_{GS} = \frac{2\pi e^2 \hbar D_{GS}}{cn_r \varepsilon_\circ m_\circ^2 v_d} \frac{|P_{cv}|^2}{E_{GS}} \frac{\xi}{\Gamma_\circ}(2P_{GS}-1) = K_{GS}(2P_{GS}-1) \quad (12)$$

$$g_{ES} = \frac{2\pi e^2 \hbar D_{ES}}{cn_r \varepsilon_\circ m_\circ^2 v_d} \frac{|P_{cv}|^2}{E_{ES}} \frac{\xi}{\Gamma_\circ}(2P_{ES}-1) = K_{ES}(2P_{ES}-1) \quad (13)$$

Note that $|P_{cv}|^2$ is the density matrix momentum. ξ is coverage factor ($\xi = V_D N_D$, N_D is photon density and V_D is volume density) and Γ_0 is non-homogeneous broadening factor , n_r is refractive index and V_d is volume of active region. In table 1 there are some constant values used in above equations.

III. Results and Tables

In this section, numerical results have been presented. **Fig.2** shows the output power as a function of coverage factor. Output power for both ground state and exited state has been calculated. Here we can clearly recognize that increasing the coverage

factor, will increase the output power in GS in fast manner at first, but after increasing for higher values of coverage factor it will increase slowly. As well as we can see output power for ES will increase suddenly, but where output power in GS start to increase in lower speed, output power for ES have a maximum and for higher values it will decrease. This is the meaning of two-state lasing in InAs/InP (113) B QD lasers. . **Fig.3.** is the diagram of output power for exited state as a function of injected bias current for three various values of cavity length. The first value is less than experimental one, the second is as same as real value used in experimental model [xxi] and the last one is more than experimental value. We have chosen these three values in this figure and other figures to compare numerical result to optimize it. Clearly, with increasing

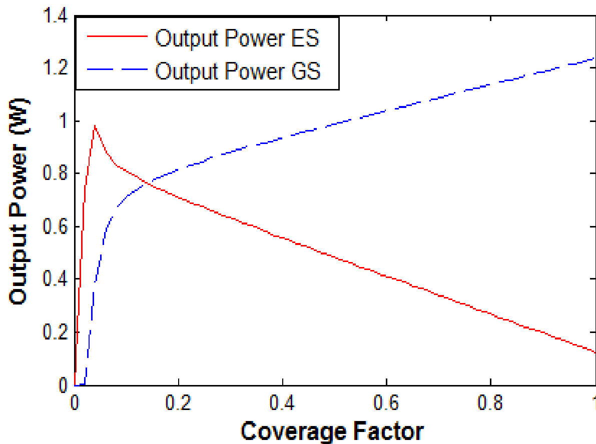

Fig.2. Output power as a function of coverage factor

Parameter	Value
Active region length	L=0.0245 cm
QD layers	N=6
Internal modal loss	$\alpha_i = 6\ cm^{-1}$
Mirror reflectivity	R1=R2=0.3
Refractive index	n_r=3.27
Spantaneous emission from WL	$\tau_{WL}^{spon} = 500\ ps$
Spantaneous emission from ES	$\tau_{ES}^{spon} = 500\ ps$
Spantaneous emission from GS	$\tau_{GS}^{spon} = 1200\ ps$
Spantaneous emission factor	$\beta_{sp} = 10^{-3}$
QD surface dendity	N_D=5*10^{10} cm^{-2}

Table.1: Constant values used in simulations

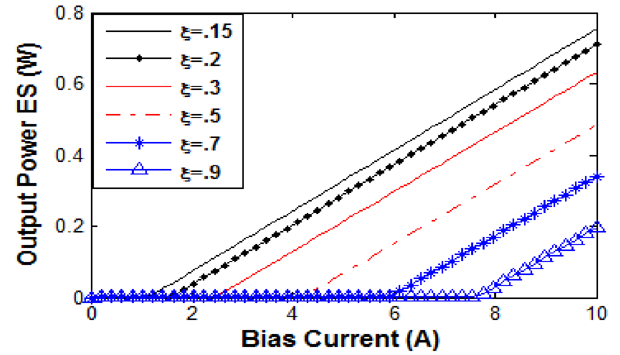

Fig.3. Output power for exited state as a function of bias current for three different value of cavity length

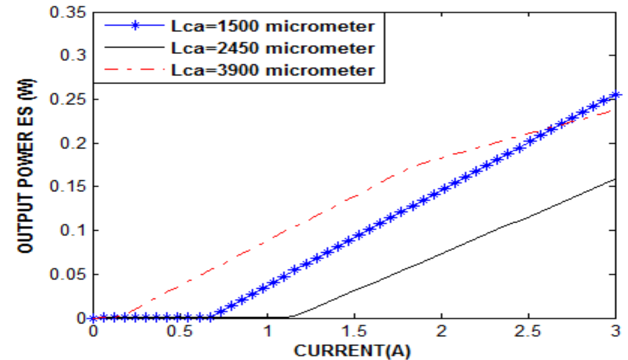

Fig.4..Output power for exited state as a function of bias current for six different value of coverage factor

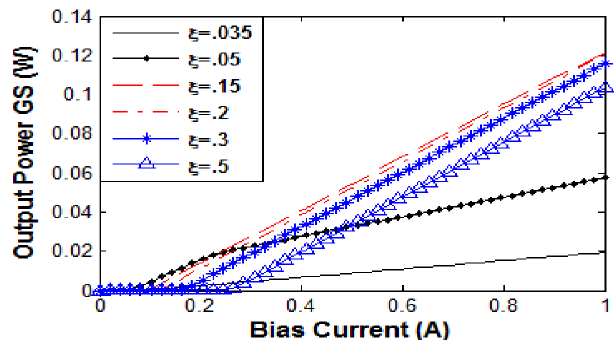

Fig.5.Output power for ground state as a function of bias current for six different value of coverage factor

cavity length, threshold injected bias current will increase too, but for more cavity length it will decrease suddenly. Also calculations show for ES with increasing cavity length out output power will decrease at first, after that for the third value it will be decreased. So we can say there is an optimized or maximum value for cavity length for lasing from ES.

Fig.4.is the same diagram shown in Fig.3 but for six various coverage factors. It's crystal clear that enhancing coverage factor threshold injected bias current will increase and output power will decrease. So for optimizing coverage factor it is better to choose the minimum possible value of it.

Now it is time to discuss about output power of ground state. Emitting photon from GS is occurred in low injected currents.Fig.5.is diagram of output power for GS for various

coverage factors. As you see threshold injected bias current will increase, but for more values of coverage factor it will decrease, however, output power will be increased.

Fig.6. is as same as Fig.5.but for different values of cavity length. It is clear that with enhancing cavity length, threshold injected bias current will increase too, however output power decreases continuously. By comparison these figures it is easy to find out for optimizing InAs/InP (113) B QD lasers for lasing both GS and ES we can consider roles of cavity length and coverage factor with each other. There is a maximum value for output power for cavity length in ES and coverage factor in GS.SO these two parameters can optimize InAs/InP (113) B QD lasers when they combine together.

Fig.7. demonstrates photon density for GS as a function of time for three different value of coverage factor. Turn on delay as an important significant is calculated here. As you see, in a constant injected bias current with enhancing cavity length turn on delay and output power from GS increase too.

In Fig.8. we have investigated photon density for GS as a function of time for six different values of coverage factors. This figure declares that with increasing of coverage factor for InAs/InP (113) B QD lasers the result will increase photon density in saturation situation until coverage factor is 0.3 .After this value it will decrease. So there is a maximum value for saturated photon density for GS. This is an evidence that is so useful and not costly to combine cavity length and coverage factor to optimize InAs/InP (113) B QD lasers.

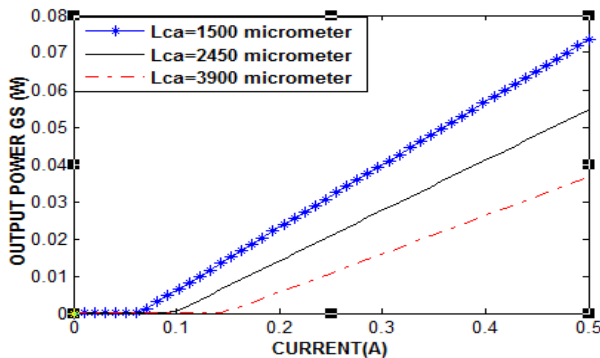

Fig.6. Output power for ground state as a function of bias current for three different value of cavity length

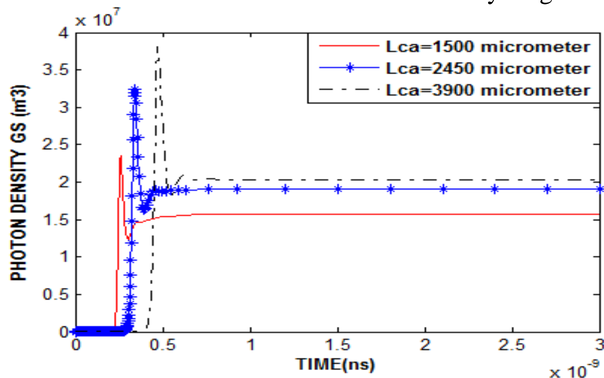

Fig.7. Photon density for exited state as a function of time for diverse cavity length

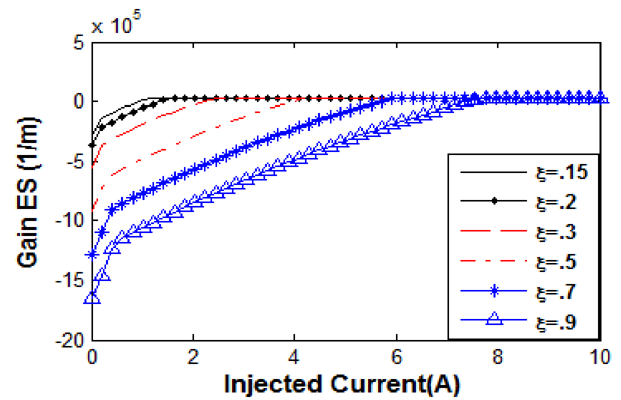

Fig.8. Photon density for exited state as a function of time for diverse coverage factors

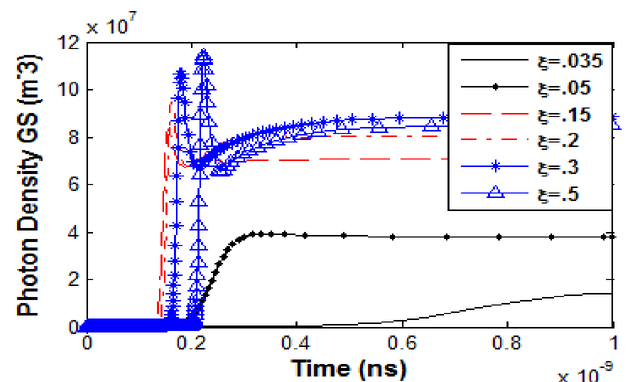

Fig.9.Optical gain for exited state as a function of injected bias current for several values of coverage factor

Finally, **Fig.5** is the diagram of optical gain for excited state as a function of bias current. It is clear that optical gain is low for QD lasers and it is one of their characteristics. It demonstrates that with increasing of coverage factor, optical gain will be saturated in higher injected bias current. This is clearly displayed optical gain will be saturated with the same value for all these six amounts of coverage factor.

IV. Conclusion

Increasing coverage factor ($\xi = V_D\, N_D$) will increase the probability of catching carriers in QD because the possibility of indwelling levels decrease ($P_{GS,ES} = {}^{N}\!/_{2\, V_D\, N_D}$). So there is a threshold coverage for carriers in order to overcome losses. With comparing the same diagrams for different values of coverage factors and cavity lengths, we can easily optimize the two state lasing InAs/InP (113) B QD lasers.

References

i. O. B. Shchekin and D. G. Deppe, "1.3 _m InAs quantum dot laser with _ _ ___ K from 0 to 80 C," Appl. Phys. Lett., vol. 80, pp.3277–3279, 2002.

ii. S. Fathpour, Z. Mi, P. Bhattacharya, A. R. Kovsh, S. S. Mikhrin, I. L. Krestnikov, A. V. Kozhukhov, and N. N. Ledentsov, "The role of Auger recombination in the temperature-dependent output

characteristics of _-doped 1.3 _m quantum dot lasers," Appl. Phys. Lett., vol. 85, pp. 5164–5166, 2004.

iii. *I. P. Marko, N. F. Masse, S. J. Sweeney, A. D. Andreev, A. R. Adams, N. Hatori, and M. Sugawara, "Carrier transport and recombination in _-doped and intrinsic 1.3 _m InAs/GaAs quantum-dot lasers," Appl. Phys. Lett., vol. 87, p. 211114, 2005.*

iv. *R. R. Alexander, D. T. D. Childs, H. Agarwal, K. M. Groom, H. Y. Liu, M. Hopkinson, R. A. Hogg, M. Ishida, T. Yamarnoto, M. Sugawara, Y. Arakawa, T. J. Badcock, R. J. Royce, and D. J. Mowbray, "Systematic study of the effects of modulation _-doping on 1.3 _m quantum-dot lasers," IEEE J. Quantum Electron., vol. 43, no. 12, pp. 1129–1139, Dec. 2007*

v. *I. C. Sandall, P. M. Smowton, J. D. Thomson, T. Badcock, D. J. Mowbray, H. Y. Liu, and M. Hopkinson, "Temperature ependence of threshold current in _-doped quantum dot lasers," Appl. Phys. Lett., vol. 89, p. 151118, 2006*

vi. *C. Y. Liu, S. F. Yoon, Q. Cao, C. Z. Tong, and H. F. Li, "Low transparency current density and high temperature operation from ten-layer p-doped 1.3 _m InAs/InGaAs/GaAs quantum dot lasers," Appl. Phys.Lett., vol. 90, p. 041103, 2007.*

vii. *Y. Arakawa and H. Sakaki, Appl. Phys. Lett., **40**, 939 (1982*

viii. *M. Sugawara, K. Mukai, H. Hhoji, Appl. Phys. Lett. 71 (19) (1997) 2791.*

ix. *A. Fiore, P. Borri, W. Langbein, et al., Appl. Phys. Lett. 80 (2002) 911.*

x. *M.C. Tatham, J.F. Ryan, C.T. Foxon, Phys. Rev. Lett. 63 (1989) 1637.*

xi. *Rui Wang, Soon Fatt Yoon, Han Xue Zhao, Cun Zhu Tong, Chong Yang Liu, and Qi Cao" Effect of inter-level relaxation and cavity length on double-state lasing performance of quantum dot lasers" Physica E 39 (2007) 203–208*

xii. *Grundmann, M., Stier, O., BognaAˆ r, S., Ribbat, C., Heinrichsdorff, F.,and Bimberg, D.: 'Optical properties of self-organized quantum dots: modelling and experiments', Phys. Stat. Sol., 2000, 178, p. 255*

xiii. *Hatori, H., Sugawara, M., Mukai, K., Nakata, Y., and Ishikawa, H.:'Room-temperature gain and differential gain characteristics of self-assembled InGaAs/GaAs quantum dots for 1.1–1.3 mm semiconductor laser', Appl. Phys. Lett., 2000, 77, (6), pp. 773–775*

xiv. *Sugawara,M., Hatori,N.,Ebe, H.,Arakawa,Y., Akiyama, T.,Otsubo, K., and Nakata, Y.: 'Modelling room-temperature lasing spectra of 1.3 mm selfassembled InAs/GaAs quantum-dot lasers: homogeneous broadening of optical gain under current injection', J. Appl. Phy., 2005, 97, p. 043523*

xv. *Markus, A., Chen, J.X., Paranthoen, C., Fiore, A., Platz, C., and Gauthier-Lafaye, O.: 'Simultaneous two-state lasing in quantum-dot lasers', Appl. Phys. Lett., 2003, 82, (12), pp. 1818–1820*

xvi. *Platz, C., Paranthoen, C., Caroff, P., Bertru, N., Labbe, C., Even, J., Dehaese, O., Folliot, H., Le Corre, A., Loualiche, S., Moreau, G., Simon, J.C., and Ramdane, A.: 'Comparison of InAs quantum dot lasers emitting at 1.55 mm under optical and electrical injection', Semicond. Sci. Technol., 2005, 20, pp. 459–463*

xvii. *K. Ludge, M. J. P. Bormann, E. Malic, P. Hovel, M. Kuntz, D. Bimberg, A. Knorr, and E. Scholl, "Turn-on dynamics and modulation response in semiconductor quantum dot lasers," Phys. Rev. B, vol. 78, pp. 35316– 35327, 2008.*

xviii. *P. Bhattacharya, S. Ghosh, S. Pradhan, J. Singh, Z. Wu, J. Urayama, K. Kim, T. Thedore, and B. Norris, "Carrier dynamics and high-speed modulation properties of tunnel injection InGaAs-GaAs quantum-dot lasers," IEEE J. Quantum Electron., vol. 39, no. 8, pp. 952–962, Aug. 2003. [18] D. G. Deppe, H. Huang, and O. B. Shchekin, "Modulation characteristics of quantum-dot lasers: The influence of p-type doping and electronic density of states on obtaining high speed," IEEE J. Quantum Electron., vol. 38, no. 12, pp. 1587–1593, Dec. 2002.*

xix. *D. G. Deppe and H. Huang, "Fermi's golden rule, nonequilibrium electron capture from the wetting layer, and the modulation response in p-doped quantum-dot lasers," IEEE J. Quantum Electron., vol. 42, no. 3, pp. 324– 330, Mar. 2006.*

xx. *D. G. Deppe and D. L. Huffaker, "Quantum dimensionality, entropy, and themodulation response of quantum dot lasers," Appl. Phys. Lett., vol. 77, pp. 3325–3327, 2000. [21] C. Z. Tong, D.W. Xu, and S. F. Yoon, "Carrier relaxation and modulation response of 1.3 μm InAs-GaAs quantum dot lasers," J. Lightw. Technol., vol. 27, pp. 5442–5450, 2009.*

xxi. *Kiril Veselinov, Frédéric Grillot, Charles Cornet, Jacky Even, Alexander Bekiarski, Mariangela Gioannini, and Slimane Loualiche "Analysis of the Double Laser Emission Occurring in 1.55-_m InAs–InP (113)B Quantum-Dot Lasers "IEEE JOURNAL OF QUANTUM ELECTRONICS, VOL. 43, NO. 9,SEPTEMBER2007*